

AN ADAPTIVE COMET METHOD

A Thesis
Presented to
The Academic Faculty

by

Kyle Eugene Remley

In Partial Fulfillment
of the Requirements for the Degree
Master of Science in Nuclear Engineering in the
George W. Woodruff School of Mechanical Engineering

Georgia Institute of Technology
May 2015

COPYRIGHT ©KYLE EUGENE REMLEY 2015

AN ADAPTIVE COMET METHOD

Approved by:

Dr. Farzad Rahnema, Advisor
Nuclear and Radiological Engineering and
Medical Physics Program,
George W. Woodruff School of Mechanical
Engineering
Georgia Institute of Technology

Dr. Dingkan Zhang
Nuclear and Radiological Engineering and
Medical Physics Program,
George W. Woodruff School of Mechanical
Engineering
Georgia Institute of Technology

Dr. Bojan Petrovic
Nuclear and Radiological Engineering and
Medical Physics Program,
George W. Woodruff School of Mechanical
Engineering
Georgia Institute of Technology

Date Approved: April 9, 2015

This thesis is dedicated to my CRMP lab mates, whose guidance and wisdom inspire and motivate me in my goal of producing vibrant and meaningful research.

ACKNOWLEDGEMENTS

I would like to express my sincere gratitude towards my advisor Dr. Farzad Rahnema for his wisdom and guidance during my graduate studies, Dr. Dingkan Zhang for his continuous support and helping me navigate the intricacies of COMET, and Dr. Bojan Petrovic for serving on my committee and for help in laying the foundation of my undergraduate education in nuclear engineering. I would also like to acknowledge the DOE Office of Nuclear Energy University Program (NEUP) for their financial support during the time of my research towards this thesis.

TABLE OF CONTENTS

| | Page |
|---|------|
| ACKNOWLEDGEMENTS | iv |
| LIST OF TABLES | vii |
| LIST OF FIGURES | viii |
| SUMMARY | ix |
| <u>CHAPTER</u> | |
| 1 Introduction | 1 |
| 2 The COMET Method | 3 |
| 2.1 Domain Decomposition | 3 |
| 2.2 Flux Expansion | 4 |
| 2.3 Solution Method | 5 |
| 3 The Adaptive Method | 8 |
| 3.1 An Adaptive Criterion | 8 |
| 3.2 Incorporating Problem-Dependent Phenomena | 10 |
| 3.3 Heuristic for Physical Insight in Truncation | 12 |
| 4 Benchmark Specifications and Computational Models | 14 |
| 4.1 C5G7 Benchmark Specification | 14 |
| 4.2 Computational Model for the C5G7 Problem | 17 |
| 4.3 PWR Core with MOX Specification | 17 |
| 4.4 Computational Model for the PWR Core with MOX Problem | 19 |
| 5 Results and Discussion | 21 |
| 5.1 Flux Expansion Results | 23 |
| 5.2 Eigenvalue and Pin Fission Density Results | 25 |

| | |
|--|----|
| 5.3 Relative Runtime Results | 27 |
| 5. 4 Comparison to Low Order Solutions | 28 |
| 6 Concluding Remarks and Future Work | 31 |
| REFERENCES | 33 |

LIST OF TABLES

| | Page |
|--|------|
| Table 1: Unique Coarse Mesh Specification for the C5G7 Problem | 17 |
| Table 2: Unique Coarse Mesh Specification for the PWR Problem | 20 |
| Table 3: Value of ε for Various Meshes | 22 |
| Table 4: Flux Expansion Results for the C5G7 Problem | 23 |
| Table 5: Flux Expansion Results for the PWR Problem | 24 |
| Table 6: Eigenvalue Agreement for the C5G7 Problem | 25 |
| Table 7: Eigenvalue Agreement for the PWR Problem | 25 |
| Table 8: Pin Fission Density Agreements for the C5G7 Problem | 26 |
| Table 9: Pin Fission Density Agreements for the PWR Problem | 26 |
| Table 10: Runtime Results for the C5G7 Problem | 27 |
| Table 11: Runtime Results for the PWR Problem | 27 |
| Table 12: Low Order COMET Eigenvalue Agreement for the C5G7 Problem | 29 |
| Table 13: Low Order COMET Eigenvalue Agreement for the PWR Problem | 29 |
| Table 14: Low Order COMET Pin Fission Density Agreements for C5G7 | 29 |
| Table 15: Low Order COMET Pin Fission Density Agreements for the PWR | 29 |
| Table 16: Low Order COMET Runtime Results for the C5G7 Problem | 30 |
| Table 17: Low Order COMET Runtime Results for the PWR Problem | 30 |

LIST OF FIGURES

| | Page |
|---|------|
| Figure 1: The Pin Cell Makeup of C5G7 | 15 |
| Figure 2: The Pin Cell Layout of the Problem | 15 |
| Figure 3: Three-Dimensional Layout | 15 |
| Figure 4: Rodded Configurations of C5G7 | 16 |
| Figure 5: Radial Core Layout with Control Rod Banks | 18 |
| Figure 6: Axial modeling of the PWR core | 19 |

SUMMARY

This thesis presents a formulation for an adaptive COMET method for solving whole reactor eigenvalue and flux distribution problems using a varying flux expansion at mesh interfaces. While COMET solutions have enjoyed accuracy on par with Monte Carlo techniques with a computational efficiency several orders of magnitude greater than stochastic methods, it was desired to extend the efficiency of the method further. Improved efficiency is obtained by allowing the flux expansion at mesh interfaces, which was previously held constant throughout a whole problem, to adapt to different expansion orders depending upon mesh composition and spatial effects due to neighboring meshes. To test the method, two benchmark problems were solved using the standard and adaptive COMET solution methods: the C5G7 benchmark problem and a pressurized water reactor benchmark with mixed-oxide (MOX) fuel assemblies. In both benchmark cases, three different configurations for different insertion of control rods were considered. For all cases, the agreement between the standard and adaptive COMET solutions was excellent, with eigenvalue agreement being 3 pcm or less and average pin fission errors being much less than 0.5% in all cases. Increases in computational efficiency by factors of 2.1 to 3.6 were observed. The strong performance of the adaptive method implies that it can be used to obtain accurate solutions to reactor problems with more efficiency than the standard COMET method.

CHAPTER 1

INTRODUCTION

The Coarse Mesh Radiation Transport, or COMET, method has been used to solve whole reactor core eigenvalue and flux distribution problems. The COMET method allows for explicit modeling of problem geometry without spatial homogenization while computing global (eigenvalue) and local (e.g., pin fission density) solutions with accuracy on par with Monte Carlo calculations. However, the method allows for calculations to be performed with formidable computational efficiency. COMET calculations are carried out in a computational runtime that is several orders of magnitude smaller than stochastic calculation runtimes.

The COMET method has been benchmarked against many different types of problems ranging many different reactor types. The method has been shown to agree very well with benchmark solutions for PWR¹, BWR¹, CANDU¹, and HTGR¹ reactor types, and, more recently, COMET has been benchmarked against novel reactor designs such as the EPR². As COMET has been shown to be an accurate and efficient computational method for reactor calculations for many different reactor types, it has presented itself as a useful design tool. As such, it is desirable to increase the computational efficiency of the method as far as possible since design is a process that requires many repeated calculations (e.g., for optimization). It is under this motivation that the work of this thesis takes place.

The major assumption of the COMET method is a flux expansion on the mesh surfaces. In the past, this expansion has been constant throughout the whole problem across all meshes. In the study of this thesis, a novel method that allows the flux expansion to vary in a problem is developed and benchmarked. Previously introduced and developed by Remley and Rahnema^{3,4}, this adaptive expansion

technique increases the computational efficiency of COMET solutions while providing only a minor detriment to its accuracy. However, previous work with the technique was limited to toy problems and small benchmark problems. In this study, the ability of the adaptive expansion technique to provide whole-core solutions with increased computational efficiency is demonstrated.

The following chapters detail the study, development, and evaluation of the adaptive expansion technique for the COMET method. Chapter 2 presents a review of the COMET method, especially the notion of a flux expansion used in its solution method. Chapter 3 details the adaptive expansion technique that has been developed. Chapter 4 discusses the benchmark problems solved. Results comparing the adaptive COMET solution to the standard COMET solution to the benchmark problems are given in chapter 5. Chapter 6 contains concluding thoughts as well as a discussion of future work.

CHAPTER 2

THE COMET METHOD

In order to describe the adaptive method put forth in this study, the COMET method is reviewed here. Emphasis is placed on the domain decomposition and flux expansion since these aspects of the COMET method motivate the adaptive technique. For a more thorough review of the COMET method, the reader is encouraged to consult the references^{5,6}.

2.1 Domain Decomposition

The steady-state distribution of the angular neutron flux in a large heterogeneous system of volume V is given by the transport equation below:

$$\begin{aligned} \hat{\Omega} \cdot \nabla \psi(\vec{r}, \hat{\Omega}, E) + \sigma(\vec{r}, E) \psi(\vec{r}, \hat{\Omega}, E) = \int_0^\infty dE' \int_{4\pi} d\hat{\Omega}' \sigma_s(\hat{\Omega}', E' \rightarrow \hat{\Omega}, E) \psi(\vec{r}, \hat{\Omega}', E') \\ + \frac{\chi(\vec{r}, E)}{4\pi k} \int_0^\infty dE' \nu \sigma_f(\vec{r}, E') \int_{4\pi} d\hat{\Omega}' \psi(\vec{r}, \hat{\Omega}', E'). \end{aligned} \quad (1)$$

The boundary condition is given by

$$\psi(\vec{r}_b, \hat{\Omega}, E) = B\psi(\vec{r}_b, \hat{\Omega}', E'), \hat{n} \cdot \hat{\Omega} < 0, \hat{n} \cdot \hat{\Omega}' > 0, \vec{r}_b \in \partial V. \quad (2)$$

Here, ψ is the angular flux, and k is the global eigenvalue. ∂V is the system boundary, and \hat{n} is the unit outward normal. B is a general boundary condition operator.

The COMET method decomposes the system volume V into non-overlapping subvolumes V_i . Each subvolume V_i is called a coarse mesh. Within each coarse mesh, the angular flux φ_i is given by the equation

$$\begin{aligned} \hat{\Omega} \cdot \nabla \varphi_i(\vec{r}, \hat{\Omega}, E) + \sigma(\vec{r}, E) \varphi_i(\vec{r}, \hat{\Omega}, E) = \int_0^\infty dE' \int_{4\pi} d\hat{\Omega}' \sigma_s(\hat{\Omega}', E' \rightarrow \hat{\Omega}, E) \varphi_i(\vec{r}, \hat{\Omega}', E') \\ + \frac{\chi(\vec{r}, E)}{4\pi k} \int_0^\infty dE' \nu \sigma_f(\vec{r}, E') \int_{4\pi} d\hat{\Omega}' \varphi_i(\vec{r}, \hat{\Omega}', E'), \end{aligned} \quad (3)$$

with the boundary condition

$$\varphi_i^-(\vec{r}_{ij}, \hat{\Omega}, E) = \varphi_j^+(\vec{r}_{ij}, \hat{\Omega}, E), \quad \vec{r}_{ij} \in \{V_i \cup V_j\} \text{ for all } V_j \text{ bounding } V_i, \quad (4)$$

where the “-” and “+” superscripts indicate incoming and outgoing angular fluxes, respectively. V_j represents all coarse meshes surrounding V_i , and φ_j is the angular flux found in coarse mesh V_j . If the coarse mesh V_i lies on a system boundary, then the following boundary condition for (3) applies:

$$\varphi_i^-(\vec{r}_{ib}, \hat{\Omega}, E) = B\varphi_i^+(\vec{r}_{ib}, \hat{\Omega}', E'), \quad \vec{r}_{ib} \in \{V_i \cup \partial V\}. \quad (5)$$

If ψ is the solution to the global problem (1-2) and k is the global eigenvalue of the system, φ_i is equal to ψ within V_i . In addition, within each local problem summarized by (3-5) the value k becomes fixed as the global value. As a result, the equations (3-5) become a coupled system of fixed-source problems.

2.2 Flux Expansion

The domain decomposition described above introduces no approximation to the global problem solution. However, since the flux is not known *a priori*, an approximation must be made in the form of a flux expansion. The expansion in each mesh is of the form

$$\varphi_i = \sum_s \sum_m J_{s,m}^{i,-} R_{s,m}^i, \quad (6)$$

where $R_{s,m}^i$ is the flux in mesh i responding to the boundary condition

$$R_{s,m}^i(\vec{r}_{is}, \hat{\Omega}^-, E) = \begin{cases} \Gamma^m(\vec{r}_{is}, \hat{\Omega}^-, E) & \text{for } \vec{r} \in \partial V_{is} \\ 0, & \text{otherwise} \end{cases} \quad (7)$$

In this equation, $\hat{\Omega}^-$ represents all angles incoming into a mesh ($\hat{n} \cdot \hat{\Omega} < 0$). Γ^m is an assumed function of orthogonal polynomials in space and angle and a delta function in energy in accordance with traditional multigroup formulation:

$$\Gamma^{ijklg} = \delta_g P_i(x) P_j(y) P_k(\mu) P_l(\phi). \quad (8)$$

The expansion coefficients $J_{s,m}^{i,+/-}$ are defined in the halfspace (“-” for incoming or “+” for outgoing) as

$$J_{s,m}^{i,+/-} = \int dE \int_{\partial V_{is}} d\vec{r} \int_{\hat{n}^{+/-} \cdot \hat{\Omega} > 0} d\hat{\Omega} (\hat{n}_{is}^{+/-} \cdot \hat{\Omega}) \varphi_i^{+/-}(\vec{r}, \hat{\Omega}, E) \Gamma^m. \quad (9)$$

Here, $\hat{n}_{is}^{+/-}$ is the outward or inward normal on surface s of mesh i . From (9), it is seen that the zeroth moment expansion coefficients are simply the incoming or outgoing partial currents of each face of each mesh. This result is the motivation for the use of notation for the expansion coefficients.

Furthermore, it is seen that if the expansion set is complete, the problem is solved via flux expansion without approximation. However, in practice, a truncation (and therefore an approximation of the problem) of the expansion must be made. Clearly, efficiency of the method relies on an expansion order that is low while maintaining a desired level of accuracy.

2.3 Solution Method

COMET calculations are two-stage. The first stage of calculation is response generation, which is performed with a stochastic method to allow for explicit geometry modeling of problems. The second stage of calculation is the deterministic sweep, which computes a solution based on the precomputed responses.

In response generation, each unique coarse mesh is modeled individually, and a fixed-source calculation as described above is carried out. The boundary condition in the transport calculation is in accordance with equation (7) above. Outgoing fluxes on each surface, which are called surface-to-surface response functions, are tallied in response to this incoming flux boundary condition. These surface-to-surface responses are defined by the equation

$$R_{ss',mm'}^i = \int dE \int_{\partial V_{is'}} d\vec{r} \int_{n^{+/-} \cdot \hat{\Omega} > 0} d\hat{\Omega} (\hat{n}_{is'}^+ \cdot \hat{\Omega}) R_{sm}^i(\vec{r}, \hat{\Omega}, E) \Gamma^{m'}. \quad (10)$$

Clearly, $R_{ss',mm'}^i$ is the flux exiting surface s in moment m for mesh i responding to an incoming flux on surface s' in moment m' . Other response quantities of interest (e.g., pin fission density values) responding to the incoming flux boundary condition are tallied as well. Such fixed source transport calculations are carried

out for an incoming flux on every surface of every mesh. Once all calculations have been carried out, the resulting responses are stored in a library.

The second stage of the calculation, the deterministic sweep, uses these precomputed responses to solve the coupled set of fixed source problems given by (3-5) above. Starting from initial guesses for both flux and global eigenvalue, the deterministic calculation consists of two layers of iterations.

Inner iterations converge flux by performing power iterations to solve the eigenvalue problem

$$\sum_{s',m'} R_{ss',mm'}^i(k) J_{s',m'}^{i,-} = \lambda J_{s,m}^{i,+}, \quad (11)$$

where the eigenvalue λ is the discontinuity factor between incoming partial current and its high moments and outgoing partial current and its high moments. For notational convenience, this eigenvalue problem can be recast as a matrix equation

$$\mathbf{R}(k) \mathbf{J}^- = \lambda \mathbf{J}^+, \quad (12)$$

where the surface-to-surface response functions (which are dependent upon k due to the domain decomposition discussed above) are put in matrix form, and incoming and outgoing partial currents are written as vectors. It should be noted that when the problem is converged in both flux and global eigenvalue k , the discontinuity factor λ is equal to unity. In fact, this is a physically intuitive result, since the outgoing flux represented by \mathbf{J}^+ must be equal to an incoming flux \mathbf{J}^- for a neighboring mesh.

Once the eigenvalue problem described in (11) and (12) has been solved in a set of inner iterations, an outer iteration updates the global eigenvalue, which is calculated by the balance equation

$$k = \frac{\int d\mathbf{w} F \psi}{L + \int d\mathbf{w} A \psi}, \quad (13)$$

where \mathbf{F} and \mathbf{A} are the fission and absorption operators, respectively, L is the system leakage, and $d\mathbf{w}$ indicates integration over the whole phase space. Both inner and outer iterations continue until flux and eigenvalue are converged.

Some important facets of the solution method should be noted here. The deterministic solver converges flux and eigenvalue for any loading of coarse meshes stored in the response library. Therefore, areas unique in composition and geometry need only be modeled in the response generation precomputation phase once. Therefore, the COMET method is uniquely suited to perform many repeated transport calculations where many different geometric makeups are possible. The method can be a good reactor design tool, where many repeated calculations are required for optimization purposes. This advantage in the method can be strengthened if computational efficiency can be further increased, where computational savings are compounded over many calculations.

CHAPTER 3

THE ADAPTIVE METHOD

In the description of the flux expansion in the previous chapter, it was mentioned that the efficiency of the COMET method relied upon a low expansion order that was still able to capture the desired accuracy of the calculation. Previous applications of the method held this expansion order fixed throughout the entire problem. In an effort to increase computational efficiency of the method, however, an adaptive expansion scheme was introduced by Remley and Rahnema^{3,4}. Different expansions for different meshes may be adaptively chosen depending upon mesh-dependent characteristics as well as problem-dependent spatial effects. In problems where some meshes can tolerate a lower expansion order than the maximum stored in the response library, then the optimal expansion order can be found for each mesh, which should lead to computational savings. The adaptive method is described in this chapter.

3.1 An Adaptive Criterion

The key to the proposed adaptive criterion is information retained in truncated flux expansions. If high-order terms only offer a relatively small contribution to the overall expansion, they can be discarded. The mathematical basis for this idea is explained through error bounding in series expansions. If an expansion is truncated after n terms, then e bounds the error of the partial sum and e_r bounds the error given by the residual between the true flux value and the infinite flux expansion. This is given in the inequality below:

$$|\varphi(\mathbf{w}) - \sum_{m=1}^n J_m^- R_m(\mathbf{w})| \leq e + e_r. \quad (14)$$

In (14), \mathbf{w} indicates the phase space within a mesh, and the summation over coarse mesh surfaces as well as surface and mesh index have been suppressed for notational convenience.

This statement of error bounding does not appear to be useful *prima facie*, since it shows the error relative to an infinite (and therefore impractical) expansion. However, if one makes the assumption that the error between the maximum expansion order in the response library and an infinite expansion is negligible (a reasonable assumption, given COMET's accuracy with these expansions), and that the residual error e_r is negligible (this is also reasonable since the infinite flux expansion solves the transport problem without approximation as discussed in chapter 2) then the error bounding inequality can be rewritten as

$$|\sum_{m=1}^N J_m^- R_m(\mathbf{w}) - \sum_{m=1}^n J_m^- R_m(\mathbf{w})| \leq e, \quad (15)$$

where N is the maximum expansion order in the database. If both sides are divided by the maximum expansion order term, then the relative error inequality

$$\left| \frac{\sum_{m=1}^n J_m^- R_m(\mathbf{w})}{\sum_{m=1}^N J_m^- R_m(\mathbf{w})} - 1 \right| \leq \varepsilon \quad (16)$$

is obtained. From this equation the adaptive criterion arises: if an expansion of order n has a sufficiently small difference ε from the maximum flux expansion of order N , then the truncation to order n is appropriate.

A feature of this method should be noted here. This adaptive criterion chooses an optimal expansion based upon a comparison with the maximum expansion. Therefore, some information about the maximum flux expansion must be known. A modification to the solution algorithm described in chapter 2 must be made.

Typical COMET solutions involve an initial guess for eigenvalue and flux, sometimes aided by low-order preconditioners and other acceleration means⁶. The solution algorithm then employs a fixed number of inner iterations followed by an outer iteration. Typically, the number of inner iterations is 150, as this has been

proven to satisfactorily converge the flux between updates in eigenvalue. However, a full set of inner iterations is not needed to provide insight into the full-ordered expansions to be used for the adaptive criterion and can slow the solution with too many full-ordered calculations, particularly with low-order preconditioning used to aid the solution algorithm. Instead, the adaptive method sets the number of inner iterations before the first outer iteration to be much smaller to a number that is chosen to be suited for the problem. After this shortened first outer iteration, the expansions for different meshes are adapted to fit the problem using the criterion described, and the flux and eigenvalue are converged through normal sets of inner and outer iterations as per the standard COMET solution algorithm.

3.2 Incorporating Problem-dependent Phenomena

Ideally, an adaptive expansion technique should take into account spatial effects when deciding to what order of expansion a mesh should be truncated. In the adaptive criterion above, the response functions are the same in any problem for a given unique coarse mesh. However, the expansion coefficients J_m^- are unique to every single mesh in a problem. These coefficients depend on problem-dependent effects such as the relative location of meshes, the size of the problem to be solved, and the imposition of boundary conditions. An obvious choice, then, is to apply the adaptive criterion to every single mesh in a problem. However, this in practice could be computationally prohibitive. For an arbitrarily large problem, the memory constraints of tracking and applying mesh-dependent data could limit the method's applicability. Therefore, in this study, the adaptive criterion is applied for each unique mesh in a problem (e.g., for each mesh that utilizes different responses). Therefore, problem dependent effects must be accounted for by incorporating averaged expansion coefficients for each unique coarse mesh. Different methods of calculating these average coefficients are discussed below.

3.2.1 Simple Averaging Method

The first manifestation of finding average-valued expansion coefficients for the adaptive criterion was to compute a simple average for expansion coefficients:

$$J_{s,m,l}^- = \frac{1}{N} \sum_i J_{s,m,l}^{-,i}. \quad (17)$$

Here, the average expansion coefficient is given for unique mesh type l for surface s in moment m . Numerical experiments have indicated that this averaging scheme has produced truncated expansions that are problem dependent based upon the effects of neighboring meshes. In addition, this method has been utilized in previous applications of the adaptive method^{3,4}. However, the simple averaging method takes into account the importance of each mesh's expansion coefficients equally. In a problem where meshes of the same type may be in very different places in a reactor (e.g., in the center and on the periphery), this uniform weighting may not provide the best insight. As a result, other average methods have been developed.

3.2.2 Current-Weighted Averaging Method

In the description of the COMET method in chapter 2, it was stated that the zeroth order expansion coefficients were simply the partial currents entering or exiting a mesh face. This can be used as a weighting method to determine average-valued expansion coefficients if the incoming partial current is used as the weighting factor:

$$J_{s,m,l}^- = \frac{\sum_i J_{s,0,l}^{-,i} J_{s,m,l}^{-,i}}{\sum_i J_{s,0,l}^{-,i}}. \quad (18)$$

Partial currents for mesh i and surface s are given by $J_{s,0,l}^{-,i}$. This method has physical justification in that meshes that are more important will have larger magnitudes of incoming partial currents entering them and thus have a more significant contribution to the averaged expansion coefficient to be used in the adaptive criterion.

3.2.3 Adjoint Weighted Averaging Method

Recently, the uncertainty quantification in COMET has been improved to include a new adjoint-based implicit correlation uncertainty analysis method⁷. This new method utilized an adjoint formulation of surface-to-surface response function defined by the following relation:

$$sR_{mm',ss'}^i = s'R_{m'm,ss'}^{*,i}. \quad (19)$$

(19) stems from the generalized reciprocity relation of the transport equation. This definition of adjoint surface-to-surface response functions is mathematically equivalent to an alternative formulation of the inner COMET problem (12):

$$\mathbf{R}^T(k)\mathbf{J}^{*,+} = \lambda\mathbf{J}^{*,-}. \quad (20)$$

Utilizing this adjoint formulation, adjoint expansion coefficients $\mathbf{J}^{*,+}$ and $\mathbf{J}^{*,-}$ can be calculated. These coefficients can then be used as a weighting function to determine average coefficients for use in the adaptive scheme as given by the equation

$$J_{s,m,l}^- = \frac{\sum_i J_{s,m,l}^{*,+,i} J_{s,m,l}^{-,i}}{\sum_i J_{s,m,l}^{*,+,i}}. \quad (21)$$

It should be noted that implementation of the adjoint-based weighting method is as of yet unclear. In previous application of the adjoint formulation in COMET solutions, the adjoint coefficients could be calculated with a few inner iterations once the forward problem had been solved. However, in this case, since truncation of expansion orders takes place before a solution of the forward problem has been computed, calculation of the adjoint coefficients is thought to be a nontrivial matter. While this weighting method has been developed from a theoretical standpoint, it is not used in numerical verification of the adaptive method. Instead, current-weighted averaging is chosen as the averaging method for all numerical results discussed in this thesis.

3.3 Heuristic for Physical Insight in Truncation

The adaptive criterion states that a relative difference of ε between a low and full-order expansion is necessary for truncation to be appropriate. However, the decision for choosing a relative difference ε is non-trivial, and it might vary for meshes of different types in a problem. Therefore, a parameter p was created to help provide physical insight in deciding the appropriate level of acceptable relative difference between a full and truncated expansion on a mesh-dependent basis. The parameter is given as

$$p = \frac{\sum_m J_m^- R_m^{NF}}{\sum_m J_m^- R_m^{AB}} - k_{guess}. \quad (22)$$

In (22), the term R_m^{NF} is the neutron production response in a mesh and R_m^{AB} is the neutron absorption response in a mesh. Both are common responses to be calculated in the building of a response library. In addition, k_{guess} is the initial guess for eigenvalue used in the deterministic phase of the COMET solution method, and the first term of (22) is the ratio of production to absorption of neutrons in a mesh. If this parameter has a large absolute value, then ε should be chosen to be small. If the parameter has a small absolute value or an absolute value equal to k_{guess} , which indicates the first term of (22) is zero and thus there is no production of neutrons in the mesh, then ε can be chosen to be a smaller value. This is because a large departure from k_{guess} , which should be close to the actual eigenvalue of the problem, could indicate the presence of large flux gradients and thus the need for a more stringent truncation criterion in some meshes. As a result, the use of (22) in conjunction with (16) provides a means of taking into account the physics of individual meshes when making the decision to truncate flux expansions. Numerical experiments have indicated that using a parameter value of 0.1 works well for most problems.

CHAPTER 4

BENCHMARK SPECIFICATIONS AND COMPUTATIONAL MODELS

Two benchmark problems were solved in this study. The first benchmark was the C5G7 problem⁸ in all its configurations. The second problem is a PWR Core with MOX^{1,9}. Both of these cores offer reactor core problems with explicit heterogeneity, and both have been solved with the COMET method in the past^{10,1}, making them good choices as benchmark problems against which to test the adaptive method.

4.1 C5G7 Benchmark Specification

The C5G7 benchmark problem is a stylized small core reactor problem with quarter-core symmetry. The problem features fuel-coolant heterogeneity, but fuel and cladding are mixed into one material. The C5G7 problem features three core configurations: Unrodded, Rodded A, and Rodded B. These configurations, as their names would imply, relate to the insertion of control rods within the core. Due to the arrangement of different control rods, the flux within the reactor will vary greatly, and the variety in possible flux gradients provides a good test for the adaptive method. While a more thorough review of the benchmark problem is given in the references⁸, a few figures describing the problem geometry are given here.

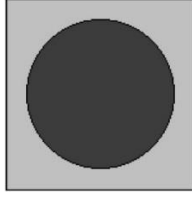


Figure 1. The Pin Cell Makeup of C5G7, taken from reference 8.

In figure 1, the darker shaded region is the fuel-clad mix and the lighter shaded region is coolant.

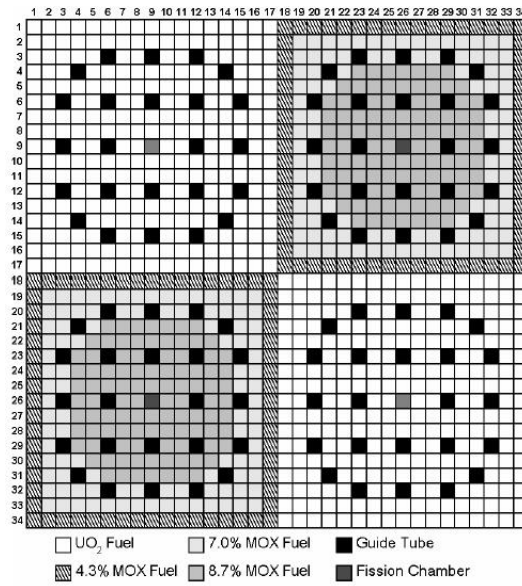


Figure 2. The Pin Cell Layout of the problem, taken from reference 8.

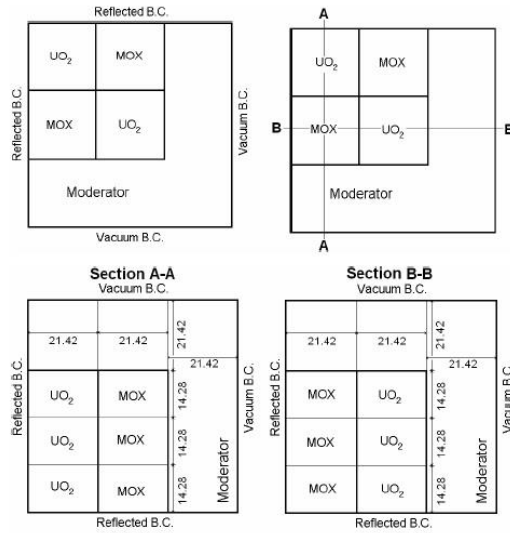


Figure 3. Three-dimensional layout, taken from reference 8. All distances are given in centimeters.

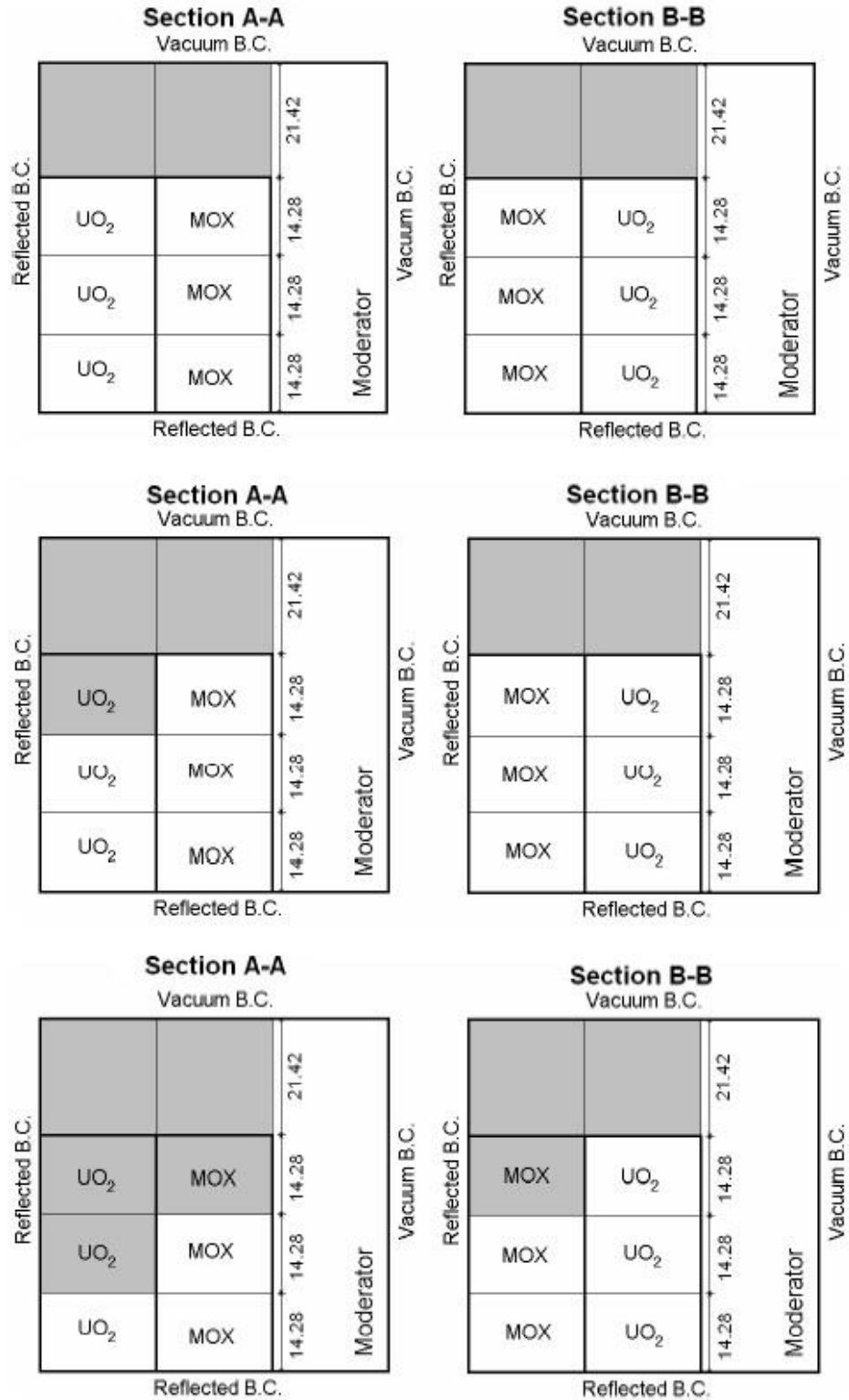


Figure 4. Rodded Configurations of C5G7, taken from reference 8.

In figure 4, shaded areas show areas with control rods inserted. The top two pictures show the Unrodded configuration, the middle two show the rodded A configuration, and the bottom two show the rodded B configuration.

4.2 Computational Model for the C5G7 Problem

Using the seven energy group cross section library specified in the benchmark, a response library consisting of fourth order expansions in both space and angle was compiled using the stochastic code MCNP5¹¹. 50 million particles were run for each case, and responses measuring surface flux, pin fission density, whole mesh neutron production, and whole mesh neutron absorption were tallied. The unique meshes specified in the model are given in the table below:

Table 1. Unique Coarse Mesh Specification for the C5G7 Problem

| Mesh | Description |
|------|-----------------------------------|
| 1 | UO ₂ Unrodded Assembly |
| 2 | UO ₂ Rodded Assembly |
| 3 | MOX Unrodded Assembly |
| 4 | MOX Rodded Assembly |
| 5 | Upper Unrodded Reflector |
| 6 | Lower Unrodded Reflector |
| 7 | Upper Rodded Reflector |

4.3 PWR Core with MOX Specification

The PWR core used in this study is a natural progression from the C5G7 problem described above. The assemblies used in this core are of the same makeup (UO₂ and MOX) as the C5G7 problem. However, this benchmark increases the complexity of the problem to be solved by increasing the modeled heterogeneity and expanding the problem size to that of a small PWR. Unlike in the C5G7 problem, Fuel, cladding, and moderator are all modeled explicitly. The core is

arranged in a checkerboard pattern between UO_2 and MOX of 121 fuel assemblies surrounded by a water reflector. A cross section of the reactor core is given below:

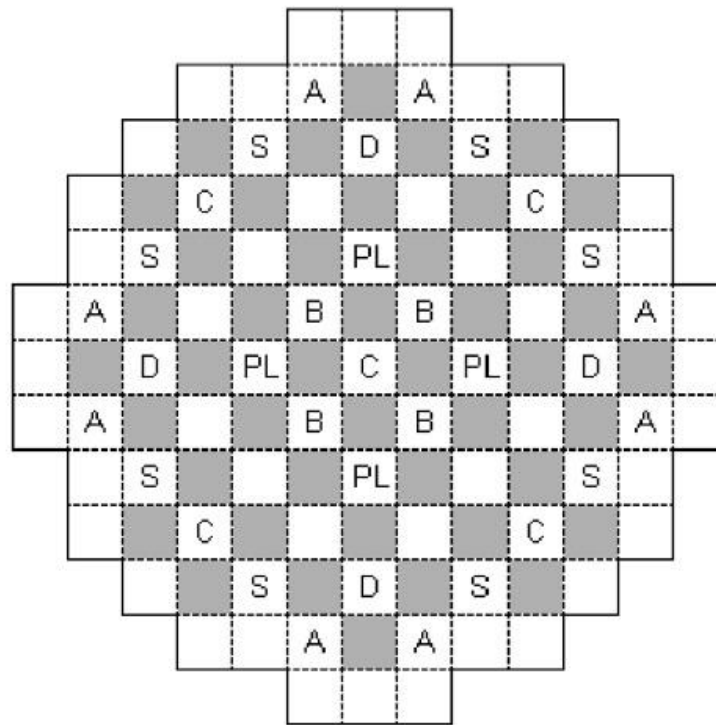


Figure 5. Radial Core Layout with Control Rod Banks, taken from reference 9

In figure 5 above, the shaded assemblies are MOX and the white assemblies are UO_2 . The symbols “A,” “B,” “C,” “D,” “S,” and “PL” indicate areas with control rods for reactivity control, shutdown, and power shaping. As specified, there are four possible assembly types in the core: UO_2 controlled, UO_2 uncontrolled, MOX controlled, and MOX uncontrolled. However, in the core configurations used in this study, UO_2 are the only assemblies that are controlled.

The three core configurations under consideration in this study are all-rods-out (ARO), all-rods-in (ARI), and some-rods-in (SRI). ARO indicates all rods are fully removed from the core, ARI indicates all rods are inserted into core locations as indicated by figure 5, and SRI indicates partial control rod insertion with the PL bank fully inserted and the D bank partially inserted with all other rods being

removed from the core. For further information on the benchmark specification, the reader is encouraged to consult the references^{1,9}.

4.4 Computational Model for the PWR with MOX Core Problem

In modeling the problem, a modification was made from the original benchmark specification given in the references. While originally the core was divided into four axial zones along the active core length, this incarnation of the benchmark problem was divided into sixteen axial zones along the active core length. This addition was to make the problem more difficult to solve and thus prove to be a more rigorous test of the adaptive COMET method and its ability to provide computational savings when core calculations can take hours. An axial profile of the core as modeled in this study is given in the figure below:

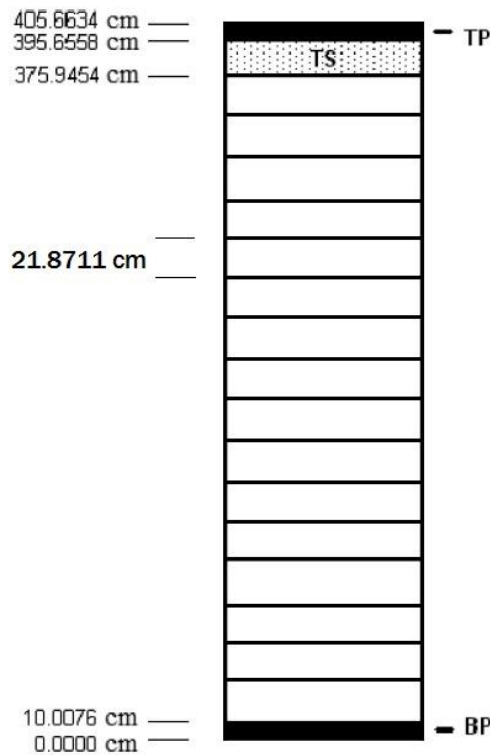


Figure 6. Axial modeling of the PWR core. The figure is modified from the one given in reference 9.

Using an eight energy group cross section library as specified in the benchmark problem description, a response library was compiled using the stochastic code MCNP5¹¹. Expansions up to fourth order in space and second order in angle were tallied for this response library, where surface flux, pin fission density, whole mesh neutron production, and whole mesh neutron absorption were the tallied responses in this model. The maximum expansion order in angle is only up to second order to be consistent with the previous COMET solution to this problem¹. In tallying each response, 50 million particles were run. A total of nine unique meshes were modeled for the problem. The meshes are given in the table below:

Table 2. Unique Coarse Mesh Specification for the PWR Problem

| Mesh | Description |
|-------------|---------------------------------------|
| 1 | UO ₂ Controlled Assembly |
| 2 | UO ₂ Uncontrolled Assembly |
| 3 | MOX Uncontrolled Assembly |
| 4 | Tube/Spring Uncontrolled Assembly |
| 5 | Tube/Spring Controlled Assembly |
| 6 | Plug Assembly |
| 7 | Active Core Reflector |
| 8 | Tube/Spring Reflector |
| 9 | Plug Reflector |

CHAPTER 5

RESULTS AND DISCUSSION

The standard COMET solutions to the problem were taken to be the benchmark against which the adaptive COMET calculations were compared in analyzing the results. This is because the focus of this study is to improve the computational efficiency of COMET while maintaining its accuracy. The standard COMET solutions for the C5G7 utilized the full 4th order expansions in both space and angle as compiled in the response library. Similarly, the standard COMET solutions for the PWR core with MOX utilized the full 4th order expansions in space and 2nd order expansions in angle as tallied by the response library for that problem.

Acceleration to the algorithm was applied in the implementation of the COMET method for this study. Both Low Order Acceleration (LOA) and Chebyshev polynomial filtering were used with the goal of improving efficiency of obtaining a solution. While these acceleration methods are explained in further detail in the references⁶, a review of the techniques is given here.

LOA serves as a preconditioner for the initial guess of a solution in both flux and eigenvalue for a COMET solution. While for whole core reactor problems, full-order calculations can take many hours to solve, lower-order solutions converge in much less time. These low order solutions, while not necessarily accurate, can serve as a good initial guess for a full order solution. Implementations of LOA can vary depending on a problem, but for the benchmarks in this study, a single set of inner iterations with an outer iteration of low order expansion (2,2,2,2 expansion

in space and angle) convergence on the solution proved to be a good preconditioner for the full-order and adaptive COMET solutions.

Chebyshev polynomial filtering accelerates eigenvalue problem power iteration numerical schemes by utilizing matrix polynomials to converge on eigenvectors quickly. Previous numerical work has shown that this polynomial filtering has allowed for the principal eigenvector to be converged upon more quickly with this method than with the standard power method.

It was found that solutions could be found in an acceptable time for the C5G7 problem without coupling to acceleration methods. However, for the full-core PWR, the size of the problem caused convergence on a solution to become unacceptably slow, so acceleration had to be used for this solution. Therefore, it is advisable to use acceleration methods in COMET calculations to ensure a converged solution is obtained. As a result, both benchmark problems utilized both LOA and Chebyshev polynomial filtering in both standard and adaptive COMET solutions for consistency in implementation of solution algorithms.

For the application of the adaptive technique in adaptive COMET solutions, values of ε chosen for various meshes are given in the table below:

Table 3. Value of ε for Various Meshes

| Mesh Type | C5G7 | PWR w/MOX |
|------------------|-------------|------------------|
| $ p \leq 0.1$ | 1.0E-4 | 1.0E-4 |
| $ p \geq 0.1$ | 1.0E-5 | 1.0E-4 |
| $ p = k_{mesh}$ | 1.0E-3 | 1.0E-3 |

Here, the value p is the parameter value from (22). The actual values for ε were chosen based off of physical insight for the problems. For instance, for a large PWR, flux gradients over a large volume might be smaller than the flux gradients of a relatively small core such as the one in the C5G7 problem. As a result, a harsher

criterion was imposed for $|p| \geq 0.1$ meshes in the C5G7 problem than the PWR problem. It can be seen, though, in both cases that a larger value of ε for meshes without neutron production ($|p| = k_{mesh}$) was appropriate. In addition, for the adaptive solutions, 10 inner iterations were performed before the adaptive criterion was applied in the C5G7 problem, and 30 inner iterations were performed before applying the adaptive criterion for the PWR problem.

5.1 Flux Expansion Results

The resultant flux expansions for the various configurations of the C5G7 problem are given in the table below. The expansion orders are given for the variables x , y , μ , and ϕ .

Table 4. Flux Expansion Results for the C5G7 Problem

| Mesh | Unrodded | Rodded A | Rodded B |
|-------------|-----------------|-----------------|-----------------|
| 1 | 4,4,4,4 | 4,4,4,4 | 4,4,4,4 |
| 2 | N/A | 4,4,2,2 | 2,2,2,2 |
| 3 | 4,4,2,2 | 4,4,4,4 | 4,4,4,4 |
| 4 | N/A | N/A | 4,4,2,2 |
| 5 | 2,2,2,2 | 2,2,2,2 | 2,2,2,2 |
| 6 | 4,4,2,2 | 4,4,2,2 | 4,4,2,2 |
| 7 | 2,2,2,2 | 2,2,2,2 | 2,2,2,2 |

It is seen that the flux expansions respond to problem-dependent changes between configurations in the C5G7 problem, demonstrating the ability of the averaged expansion coefficients to affect the results of the adaptive criterion. It is also seen that the adaptive criterion results in flux expansions that are reasonable given physical expectations. For instance, a higher expansion in the reflector areas next to the fuel rods (Mesh 6) is appropriate given the expected higher flux gradients there than in the reflector areas above the fuel rods (Meshes 5 and 7). Many meshes, also, can tolerate a lower expansion in angle given that the C5G7

problem models a reactor of PWR type, where anisotropy of angular flux is expected to be low. Full expansions are chosen where flux gradients are expected to be large, especially given control rod insertion in the Rodded A and Rodded B cases.

The PWR problem flux expansion results are given in the table below. As in the previous table, the expansion orders provided are for expansions in x , y , μ , and ϕ .

Table 5. Flux Expansion Results for the PWR Problem

| Mesh | ARO | SRI | ARI |
|-------------|------------|------------|------------|
| 1 | N/A | 4,4,2,2 | 4,4,2,2 |
| 2 | 4,4,2,2 | 4,4,2,2 | 4,4,2,2 |
| 3 | 2,2,2,2 | 4,4,2,2 | 4,4,2,2 |
| 4 | 2,2,2,2 | 2,2,2,2 | 2,2,2,2 |
| 5 | 2,2,2,2 | 2,2,2,2 | 2,2,2,2 |
| 6 | 2,2,2,2 | 2,2,2,2 | 2,2,2,2 |
| 7 | 2,2,2,2 | 2,2,2,2 | 2,2,2,2 |
| 8 | 2,2,2,2 | 2,2,2,2 | 2,2,2,2 |
| 9 | 4,4,2,2 | 4,4,2,2 | 2,2,2,2 |

As was seen with the flux expansion results in the C5G7 problem, flux expansions for different meshes (in this case, meshes 3 and 9) changes depending upon problem-dependent information. In addition, the flux expansions once again are appropriate given physical expectations. Higher flux gradients in the core for rodged core configurations necessitate higher expansions, for instance. In addition, it is expected that flux gradients in the reflector region are smaller for a large PWR problem such as this, so the full 2nd order expansion for many of the reflector regions seems appropriate as well.

5.2 Eigenvalue and Pin Fission Density Results

In all cases for both benchmark problems, the agreement between standard and adaptive COMET solutions was excellent. The eigenvalue agreement results for the C5G7 and PWR problems are given in tables 6 and 7 below.

Table 6. Eigenvalue Agreement for the C5G7 Problem

| | Unrodded | | Rodded A | | Rodded B | |
|-----------|----------|----------|----------|----------|----------|----------|
| | Standard | Adaptive | Standard | Adaptive | Standard | Adaptive |
| k_{eff} | 1.14335 | 1.14335 | 1.12840 | 1.12842 | 1.07798 | 1.07801 |
| (+/-) | 0.00006 | 0.00006 | 0.00006 | 0.00006 | 0.00005 | 0.00005 |
| Diff. | 0.00001 | | 0.00001 | | 0.00003 | |
| (+/-) | 0.00008 | | 0.00008 | | 0.00007 | |

Table 7. Eigenvalue Agreement for the PWR Problem

| | ARO | | SRI | | ARI | |
|-----------|----------|----------|----------|----------|----------|----------|
| | Standard | Adaptive | Standard | Adaptive | Standard | Adaptive |
| k_{eff} | 1.02011 | 1.02011 | 0.99784 | 0.99785 | 0.93621 | 0.93622 |
| (+/-) | 0.000004 | 0.000004 | 0.000004 | 0.000004 | 0.000005 | 0.000004 |
| Diff. | 0.00000 | | 0.00001 | | 0.00001 | |
| (+/-) | 0.000005 | | 0.000005 | | 0.000006 | |

From the tables above, it can be seen that the eigenvalue error for the adaptive method is small; the highest error is 3 pcm for the Rodded B configuration of the C5G7 problem, and even then, the error is less than the combined uncertainty of the results. For the PWR problem, the errors in eigenvalue are either 1 pcm or are negligible.

For measuring pin fission density agreement, several statistical measures of error were used. The error (E), average error (AE), mean relative error (MRE), root mean square error (RMSE), and maximum error (ME) are defined below:

$$E_i = \left| \frac{FD_s^i - FD_a^i}{FD_s^i} \right|, \quad (23)$$

$$AE = \frac{1}{n} \sum_i E_i, \quad (24)$$

$$MRE = \frac{\sum_i E_i FD_s^i}{\sum_i FD_i}, \quad (25)$$

$$RMSE = \sqrt{\frac{1}{n} \sum_i E_i^2}, \quad (26)$$

$$ME = \text{MAX}_i(E_i). \quad (27)$$

Using these statistical measures, the pin fission density agreements were calculated and are summarized in tables 8 and 9 below:

Table 8. Pin Fission Density Agreements for the C5G7 Problem

| Error (%) | Unrodded | Rodded A | Rodded B |
|------------------|-----------------|-----------------|-----------------|
| AE | 0.18 | 0.16 | 0.24 |
| MRE | 0.11 | 0.082 | 0.14 |
| RMSE | 0.35 | 0.32 | 0.45 |
| ME | 2.0 | 1.8 | 2.0 |

Table 9. Pin Fission Density Agreements for the PWR Problem

| Error (%) | ARO | SRI | ARI |
|------------------|------------|------------|------------|
| AE | 0.28 | 0.15 | 0.18 |
| MRE | 0.18 | 0.080 | 0.076 |
| RMSE | 0.63 | 0.55 | 0.55 |
| ME | 9.0 | 8.8 | 8.4 |

In addition, the average pin fission density uncertainties were 0.07% for the C5G7 cases. The average pin fission density uncertainties were 0.05% for the PWR cases. In all cases, the maximum pin fission density uncertainty was 0.1%.

The pin fission density agreement between the standard and adaptive COMET solutions to these benchmarks is excellent. The average pin fission density

errors are much less than 1%. The maximum errors for the PWR case are high, but this occurred on the periphery of the core, where small flux values can cause relative errors such as the ones used to grow large. In addition, the effects of the low-order parts of adaptive solutions incorporate some flux error that can be seen at the periphery.

5.3 Relative Runtime Results

In all configurations of both benchmark problems, the adaptive COMET solution was obtained with much greater computational efficiency than the standard COMET solution. All cases were run on the 2 GHz processors, so the runtime comparisons are made with the same hardware. Runtime results are given in tables 10 and 11.

Table 10. Runtime Results for the C5G7 Problem

| | Unrodded | | Rodded A | | Rodded B | |
|----------------|-----------------|-----------------|-----------------|-----------------|-----------------|-----------------|
| | Standard | Adaptive | Standard | Adaptive | Standard | Adaptive |
| Runtime | 35 min | 14 min | 36 min | 10 min | 40 min | 16 min |
| Speedup Factor | 2.5 | | 3.6 | | 2.5 | |

Table 11. Runtime Results for the PWR Problem

| | ARO | | SRI | | ARI | |
|----------------|-----------------|-----------------|-----------------|-----------------|-----------------|-----------------|
| | Standard | Adaptive | Standard | Adaptive | Standard | Adaptive |
| Runtime | 13 h | 4.0 h | 13 h | 6.0 h | 13 h | 5.7 h |
| Speedup Factor | 3.25 | | 2.1 | | 2.3 | |

Here, the speedup factor is defined by

$$Speedup\ Factor = \frac{\tau^{std}}{\tau^{ada}}, \quad (28)$$

where T^{std} is the runtime for the standard COMET solution and T^{ada} is the runtime for the adaptive COMET solution.

From the results tabulated above, it is seen that at little cost to accuracy, the adaptive COMET solutions produce results with greatly increased computational efficiency. In all cases solutions were obtained 2.1-3.6 times faster with the adaptive method.

Some observations about the convergence behavior should be noted here. In previous work with the adaptive method, the smoothing iterations at times slowed the convergence of the COMET solution, reducing computational efficiency of the adaptive method. This was remedied by varying the number of the inner iterations between every outer iteration in COMET solutions⁴. However, with the coupling to LOA and Chebyshev polynomial filtering in this study, this modification was no longer needed, as convergence of adaptive COMET solutions remained satisfactory in all cases. Further, for the PWR benchmark cases, the adaptive COMET solutions were obtained in both fewer inner and fewer outer iterations than the standard COMET solutions. This suggests that coupling to acceleration methods is an effective way of implementing the adaptive COMET method.

5.4 Comparison to Low Order Solutions

As a point of reference, the benchmark cases were solved with the standard COMET method employing a low order expansion. In all benchmark cases, this expansion was 2nd order in both space and angle. The eigenvalue and pin fission density agreements between the low order and high order COMET solutions as well as relative computational efficiencies of solutions are presented in the tables below. It should be noted that the average and maximum uncertainties in the pin fission density values are the same as the results for the adaptive and standard COMET results presented above.

Table 12. Low Order COMET Eigenvalue Agreement for the C5G7 Problem

| | Unrodded | | Rodded A | | Rodded B | |
|-----------|-----------------|------------|-----------------|------------|-----------------|------------|
| | High | Low | High | Low | High | Low |
| k_{eff} | 1.14335 | 1.14338 | 1.12840 | 1.12855 | 1.07798 | 1.07817 |
| (+/-) | 0.00006 | 0.00006 | 0.00006 | 0.00006 | 0.00005 | 0.00005 |
| Diff. | 0.00013 | | 0.00015 | | 0.00020 | |
| (+/-) | 0.00008 | | 0.00008 | | 0.00007 | |

Table 13. Low Order COMET Eigenvalue Agreement for the PWR Problem

| | ARO | | SRI | | ARI | |
|-----------|-------------|------------|-------------|------------|-------------|------------|
| | High | Low | High | Low | High | Low |
| k_{eff} | 1.02011 | 1.02014 | 0.99784 | 0.99787 | 0.93621 | 0.93618 |
| (+/-) | 0.000004 | 0.000004 | 0.000004 | 0.000004 | 0.000005 | 0.000004 |
| Diff. | 0.00003 | | 0.00003 | | 0.00003 | |
| (+/-) | 0.000005 | | 0.000005 | | 0.000006 | |

Table 14. Low Order COMET Pin Fission Density Agreement for C5G7

| Error (%) | Unrodded | Rodded A | Rodded B |
|------------------|-----------------|-----------------|-----------------|
| AE | 1.0 | 1.0 | 1.2 |
| MRE | 0.70 | 0.72 | 0.86 |
| RMSE | 1.6 | 1.6 | 1.7 |
| ME | 7.8 | 7.9 | 8.8 |

Table 15. Low Order COMET Pin Fission Density Agreement for the PWR

| Error (%) | ARO | SRI | ARI |
|------------------|------------|------------|------------|
| AE | 0.48 | 0.50 | 0.62 |
| MRE | 0.29 | 0.33 | 0.35 |
| RMSE | 0.88 | 0.89 | 0.97 |
| ME | 10.2 | 10.1 | 9.9 |

Table 16. Low Order COMET Runtime Results for the C5G7 Problem

| | Unrodded | | Rodded A | | Rodded B | |
|----------------|-----------------|------------|-----------------|------------|-----------------|------------|
| | High | Low | High | Low | High | Low |
| Runtime | 35 min | 2.4 min | 36 min | 3 min | 40 min | 2.6 min |
| Speedup Factor | 14 | | 12 | | 16 | |

Table 17. Low Order COMET Runtime Results for the PWR Problem

| | ARO | | SRI | | ARI | |
|----------------|-------------|------------|-------------|------------|-------------|------------|
| | High | Low | High | Low | High | Low |
| Runtime | 13 h | 2.1 h | 13 h | 4.1 h | 13 h | 3.6 h |
| Speedup Factor | 6.1 | | 3.2 | | 3.6 | |

The results given in the tables above demonstrate that simply using a low order standard COMET solution results in calculations that are performed with much greater computational efficiency than both the high order standard COMET and adaptive COMET solutions. However, it should be noted that in every case, the adaptive COMET solution is more accurate than the low order standard COMET solution. In all cases, the adaptive COMET solution produced results that had satisfactory accuracy of solution. However, the low order standard COMET solution, while providing decent results in the PWR case, suffered in accuracy much more in the C5G7 problem, particularly in calculating pin fission density values. It is seen, then, that simply using low order COMET solutions, while fast, is not necessarily adequate in finding an accurate solution.

CHAPTER 6

CONCLUDING THOUGHTS AND FUTURE WORK

As noted previously, the adaptive COMET solutions were able to preserve the accuracy of the standard COMET solutions while increasing computational efficiency in finding solutions. The eigenvalue agreement in all cases was within 3 pcm, and the average pin fission density errors were all much less than 0.5% while achieving speedup factors between 2.1 and 3.6.

In addition, while the low order COMET solutions provided speedup factors as high as 16, the adaptive COMET solutions proved to compare more favorably in accuracy than the low order standard COMET solutions. Eigenvalue errors are as high as 20 pcm and average pin fission density errors are as high as 1.2%. This suggests that the adaptive COMET method can be used to perform COMET calculations more efficiently and can more reliably provide accurate results than simply using low order COMET solutions. This is especially useful when many accurate reactor calculations are required, such as for optimization and design studies (e.g., control rod worth studies).

It should be noted that high maximum pin fission density errors arise with the advent of large problems. In the scope of this study, the only way to remedy these high maximum errors was to perform a full high-order standard COMET solution. While other ways to remedy these errors can be a focus of future work, a conclusion of this study is that the adaptive COMET method is accurate and efficient for many cases, but a high order COMET solution is desired if periphery flux errors should be resolved.

Another benefit of the adaptive COMET method is that it allows for COMET calculations to be performed while limiting the need for user intuition in finding a

solution. Standard COMET solutions require a heuristic knowledge of an optimal expansion order to find an adequate solution. The automated nature of finding expansion orders on a problem-dependent basis in which the adaptive COMET method no longer requires this intuition, provided the response library is sufficiently high-ordered. It should be noted that parameters such as ε values and the number of smoothing iterations at the beginning of an adaptive COMET solution were the result of tuning and should be more appropriately chosen in the future to limit the need for user intuition further.

Another aspect of future work is the inclusion of the adjoint-weighted averaging scheme for expansion coefficients in the adaptive method. Due to the properties of adjoint flux, this change to the method is expected to improve the discerning abilities of the adaptive criterion.

Further, future work should include a further study of the coupling effects of acceleration methods to adaptive COMET solutions. In this work, the acceleration coupling helped improve the convergence behavior for both benchmark cases. However, it is unclear how these acceleration methods affect adaptive COMET solutions in all cases. Other benchmark problems, possibly of different reactor types (e.g., BWR, CANDU) should be solved with the adaptive method to investigate these possible coupling effects.

REFERENCES

- [1] RAHNEMA, F., ZHANG, D. and CONNOLLY, K., “The COMET method for reactor physics calculations,” PBNC2014-099, Presented at the Pacific Basin Nuclear Conference, Vancouver, British Columbia, Canada, August 24-28 2014.
- [2] LAGO, D. “Benchmarking the Course Mesh Transport (COMET) Method.” Nuclear and Radiological Engineering/Medical Physics. Atlanta, GA. Georgia Institute of Technology. December 2013.
- [3] REMLEY, K. AND RAHNEMA, F., “Fuel pin problem solution via an accelerated COMET method,” Transactions of the American Nuclear Society, Presented at the American Nuclear Society Winter Meeting, Anaheim, CA, November 9-13 2014.
- [4] REMLEY, K. AND RAHNEMA, F., “An adaptive COMET solution to a configuration of the C5G7 benchmark problem,” ANS MC2015 - Joint International Conference on Mathematics and Computation (M&C), Supercomputing in Nuclear Applications (SNA) and the Monte Carlo (MC) Method, Presented at ANS MC2015, Nashville, TN, April 19-23 2015.
- [5] MOSHER, S. AND RAHNEMA, F., “The Incident Flux Response Expansion Method for Heterogeneous Coarse Mesh Transport Problems,” Transport Theory and Statistical Physics, vol. 35(1), pp. 55-96, 2006.
- [6] ZHANG, D. AND RAHNEMA, F., “An Efficient Stochastic/Deterministic Coarse Mesh Neutron Transport Method,” Annals of Nuclear Energy, vol. 41(1), pp. 1-11, 2012.
- [7] ZHANG, D. AND RAHNEMA, F., “An Implicit Correlation Method for COMET Core Eigenvalue Uncertainty Analysis,” Nuclear Science and Engineering, submitted in 2015.

- [8] SMITH, M., LEWIS, E., AND NA, B., Benchmark on Deterministic Transport Calculations Without Spatial Homogenization: MOX Fuel Assembly 3-D Extension Case, OECD/NEA Report NEA/NSC/DOC, Paris, France, 2005.
- [9] RAHNEMA, F. HON, R., AND DOUGLASS, S., “A Stylized Three-Dimensional Pressurized Water Reactor Benchmark Problem with UO_2 and MOX Fuel,” Nuclear Technology, vol. 183 pp. 1-28 (2013).
- [10] FORGET, B. AND RAHNEMA, F., “COMET Solutions to the 3-D C5G7 Benchmark Problem,” Progress in Nuclear Energy, vol. 48(5) pp. 467-475, 2005.
- [11] X-5 MONTE CARLO TEAM, MCNP – A General N-Particle Transport Code, Version 5, Los Alamos National Laboratory, Los Alamos, New Mexico, 2005.